Journal of Mathematical Chemistry 10(1992)313–327

EMBEDDED UNITS IN CONJUGATED POLYMERS

Jenö KÜRTI
Department of Atomic Physics, Eötvös University, Puskin u. 5–7, H-1088 Budapest, Hungary

and

Péter R. SURJÁN
Department of Theoretical Chemistry, Eötvös University, Pázmány P. sétány 1, and
Institute of Physics, Technical University, Budafoki út 8, H-1521 Budapest, Hungary

Abstract

The problem of embedding of several monomeric units (benzene, thiophene, isothianaphthene) into linear oligoenes or into a polymer built up by the same units is discussed. Using a simple model Hamiltonian, we evaluate the geometry (bond lengths) and electronic structure (energy gaps) of conjugated oligomers containing up to 200 atoms. Special attention is paid to end effects. The quinoid–aromatic transition and the conjugation interruption due to embedded defects is studied in some detail.

1. Introduction: Conjugated polymers and the embedding problem

The interaction between defects and unit cells in (quasi)periodic systems is an important issue. Such problems can be approached from different directions. In the spirit of the present volume, we shall discuss these questions from the point of view of embedding. A given unit cell and, especially, a foreign unit or defect can be considered as being embedded into a field of other cells.

The structure of unit cells or other units embedded in crystals or polymers is affected by the environment. In most cases this effect is small, the embedded unit can easily be identified and its structure in situ is only slightly different from its structure in vacuo. In other cases, the medium can force a qualitative change in the structure of the embedded units. Depending on the nature of the problem, the relevant effective interactions can be of short- or long-range character. The radius of long-range interactions can be several dozens or hundreds of atoms. Such situations typically occur if the embedded unit provides two or more significantly different structures which are (quasi)degenerate in energy. In this paper (sections 3–5), we shall provide examples for these situations by analysing the embedding of heterocyclic units, thiophene and thianaphthene, into its own polymer and polyacetylene.

An embedded unit, on the other hand, as a defect, modifies the structure of the host polymer. For example, it may lead to a (partial) interruption of conjugation.

The extent of this interruption will be studied quantitatively for phenylene, embedded in polyacetylene in various forms (ortho, meta and para) in section 6.

Organic conjugated polymers have recently received much interest due to their unusual electric, electrochemical, thermodynamic, nonlinear optical properties [1–5]. Extensive research is also stimulated by the hope of industrial applications. The prototype of such materials is polyacetylene, $(CH)_x$, which is an insulator with an energy gap of about 1.5 eV in pure form, but becomes metallic after heavy doping with cations or anions [6,7]. The highest achieved room temperature conductivity for doped *trans*-polyacetylene was reported to be more than 10^5 S/cm [8,9], which approaches the conductivity of copper.

Many properties of conjugated polymers are determined by the π-electrons delocalized over the chains. The one-dimensional character of these systems has important consequences: the delocalization due to conjugation does not lead to metallic behaviour in the pristine form of the polymers. As a matter of fact, the metallic state in one dimension is unstable against distortions in the geometry. This is the well-known Peierls instability [10]. For example, in the case of $(CH)_x$ a metallic system would emerge if the length of all C–C bonds were the same. This is not the case however, since the energetics favour alternating C–C bonds. This is supported by various theoretical models [11] and experimental observations [12,13]. It should be pointed out that the difference between long and short bond lengths is smaller than the difference between true single (e.g. in ethene) and double (e.g. in ethylene) bonds. The dimerization of the unit cell opens a gap at the Fermi level, making the material an insulator (semiconductor). It can be shown that a larger alternation produces a larger gap. We note, however, that intercalating foreign ions – doping – produces an insulator–metal transition not only in $(CH)_x$ as mentioned above, but in many other representatives of conjugated 1D polymers. The gaps of these polymers in pristine form vary within a wide range up to several eV's. The smallest gap so far (1.0 eV) has been observed for a heterocyclic polymer, named poly-isothianaphthene (PITN) [14].

Trans-polyacetylene is not only the simplest conjugated polymer, but due to its degenerate ground state opens the possibility of a unique nonlinear excitation, a soliton. For the infinite chain, the total energy is the same for the two possible orderings of the short and long bonds. A soliton (or antisoliton) is a topological defect which separates two such domains, as illustrated in fig. 1. In reality, the

Fig. 1. Soliton, a topological defect in *trans*-polyacetylene.

transition is not so sharp but extends over more than ten carbon atoms [11,15]. In the energy band structure, a soliton-type elementary excitation corresponds to a midgap state.

Finite oligomers show similar behaviour as the infinite polymers. Of course, in this case there are discrete energy levels instead of continuous bands. The first electronic excitation energy (HOMO–LUMO transition in the one-electron molecular orbital picture) corresponds to the energy gap of the solid-state limit. The bond alternation pattern is affected by the chain end effect. The geometry as well as the transition energies depend on the length of the oligomer. An important fact is that for a finite linear oligoene $CH_2-(CH)_{n-2}-CH_2$ with odd n, there is a midgap energy level and a soliton-like topological defect in the middle of the chain.

2. Models and methods

A realistic study on the structure of conjugated polymers is computationally very demanding. Understanding of real samples usually requires the study of large aperiodic clusters. This excludes the possibility of utilizing translational symmetry to simplify the calculations. Due to the size of the clusters, calculations by sophisticated quantum chemical methods (ab initio or all-valence electron semi-empirical schemes) are prohibitive. One has to turn to more flexible models which are simple enough to make the calculations manageable but accurate enough to provide reliable information on the structural parameters and energetics of the polymeric system in question.

In our laboratory, we have developed a simple model which meets the above two requirements [15–21]. The model originates from earlier work of Longuet-Higgins and Salem [22]. This is an extension of the Hückel scheme in which the usual one-electron Hamiltonian of the π-electrons is augmented by an empirical potential for the σ-electrons. The Hückel β-integrals are related to the corresponding bond length by an exponential formula. The σ-potential is determined by the requirements of Coulson's empirical bond order–bond length relationship. The method will be outlined below. A brief summary can be found in refs. [18,21].

Working with planar systems, we assume the validity of the $\sigma-\pi$ separation. The π-electrons are treated explicitly within the independent electron (Hückel) scheme. The effect of σ-electrons is implicit: they give rise to an additive σ-potential. Both the π-electron Hamiltonian and the σ-potential depend on the actual bond lengths of the molecule, which leads to a coupling between these two systems.

As usual in the Hückel scheme, we deal with one atomic orbital per site, and the π-electron molecular orbitals are expanded as

$$\phi_i(\boldsymbol{r}) = \sum_{j=1}^{N} C_j^{(i)} \cdot \chi_j(\boldsymbol{r}). \tag{1}$$

The $\chi(\boldsymbol{r})$ atomic orbitals are the p_z orbitals perpendicular to the molecular plane and are orthogonal to each other. The π-electron Hamiltonian $\hat{H}_\pi$ is represented by an $N \times N$ matrix with α_j diagonal and $\beta_{kl} \equiv \beta_{lk}$ off-diagonal elements. The MO energies can be expressed as:

$$\varepsilon_i = \langle \phi_i | \hat{H}_\pi | \phi_i \rangle = \sum_j \alpha_j C_j^{(i)*} C_j^{(i)} + \sum_{k>l} \beta_{kl} \left(C_k^{(i)*} C_l^{(i)} + C_l^{(i)*} C_k^{(i)} \right). \tag{2}$$

The total π-electron energy in the above approximation is the sum of the one-electron energies ε_i weighted by the occupation number of the corresponding molecular orbital ($n_i = 0$, 1 or 2 and $\sum_i n_i = N_\pi$):

$$E_{\pi,\mathrm{tot}} = \sum_i \varepsilon_i n_i = \sum_{\substack{j \\ (\mathrm{atoms})}} \alpha_j q_j + 2 \sum_{\substack{m \\ (\mathrm{bonds})}} \beta_m p_m, \tag{3}$$

where the following abbreviations were introduced:

$$q_i = \sum_i C_j^{(i)*} C_j^{(i)} \cdot n_i \tag{4}$$

is the π-charge for the jth atom and

$$p_m = \frac{1}{2} \sum_i \left(C_k^{(i)*} C_l^{(i)} + C_l^{(i)*} C_k^{(i)} \right) n_i \tag{5}$$

is the π-bond order for the mth bond which is formed between the kth and lth atoms (diagonal and off-diagonal elements of the π-electron density matrix). The p_m is 0 and 1 for a pure single bond and double bond (ethylene), respectively, and falls between these values in the general case. For fixed occupation numbers, $E_{\pi,\mathrm{tot}}$ is a first-order homogeneous function of α_j's and β_m's, from which, together with eq. (3), it immediately follows that

$$q_j = \frac{\partial E_{\pi,\mathrm{tot}}}{\partial \alpha_j} \quad \text{and} \quad p_m = \frac{1}{2} \frac{\partial E_{\pi,\mathrm{tot}}}{\partial \beta_m}. \tag{6}$$

So far, the results are well known in the usual Hückel theory. Longuet-Higgins and Salem generalized the Hückel theory by including the σ-electrons (σ-compressibility) and by allowing a change in the resonance integral β with changing bond length assuming a well-defined monotonic correspondence between them. Thus, in the LHS model:

$$E_{\mathrm{tot}} = E_{\pi,\mathrm{tot}}(\{r\}) + E_{\sigma,\mathrm{tot}}(\{r\}), \tag{7}$$

where

$$E_{\pi,\mathrm{tot}} = E_{\pi,\mathrm{tot}}(\alpha_1, \ldots; \beta_1(r_1) \ldots; \{n\}), \tag{8}$$

according to eq. (3), and

$$E_{\sigma,\mathrm{tot}} = \sum_m f_m(r_m). \tag{9}$$

In eq. (8), $\{n\}$ is the set of the occupation numbers. In eq. (9), $f(r)$ is the potential energy of the σ-core.

The $\beta(r)$ can be reasonably assumed as an exponential function [23]:

$$\beta(r) = -A \exp\left(-\frac{r}{B}\right). \tag{10}$$

$f(r)$ can be obtained from ground-state equilibrium considerations. The first derivatives of the total energy are zero at the equilibrium geometry:

$$\frac{\partial E_{\text{tot}}}{\partial r_m} = \frac{\mathrm{d} f_m}{\mathrm{d} r_m} + \frac{\partial E_{\pi,\text{tot}}}{\partial \beta_m} \frac{\mathrm{d} \beta_m}{\mathrm{d} r_m} = 0. \tag{11}$$

Using eq. (10) and eq. (6), from eq. (11) it immediately follows that there is a one-to-one correspondence between bond length r and bond order p. Assuming the empirically observed *linear* bond length–bond order relation (Coulson relation) [24]

$$r = R_1 - (R_1 - R_2)p \tag{12}$$

as exact, the $f(r)$ function can be obtained from eqs. (10), (11) and (12):

$$f(r) = \frac{2}{R_1 - R_2} \beta(r)(r - R_1 + B). \tag{13}$$

R_1 and R_2 are the lengths of a pure single and double bond, respectively. Even though $f(r)$ is obtained from a ground state configuration, one can use this function for all π-excitations as well because of the assumed σ–π separation. The LHS model is characterized by eqs. (7), (10) and (12) or (13).

The model needs an iterative self-consistent solution which provides optimized bond lengths by satisfying the Coulson relation, which at the same time minimizes the total energy. The procedure is illustrated in fig. 2. Assuming an initial guess

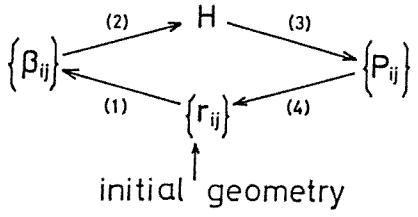

Fig. 2. Iterative solution of the LHS model.

for the bond lengths, one evaluates the resonance integrals (1) and constructs the Hamiltonian matrix (2), which is then diagonalized and the bond orders are evaluated (3). After that, the bond lengths are changed to decrease the total energy (4) and with the new bond lengths, new resonance integrals are evaluated and the procedure is repeated until convergence.

We mention that with the LHS model it is straightforward to describe, e.g., the appearance of bond alternation in linear chains as well as topological defects such as solitons or polarons [15, 19]. Calculations with similar models were performed by Julg et al. [25], László and Julg [26], and Biczó et al. [27].

There are five parameters in the model (R_1, R_2, A, B and α) for each type of bonds or atoms. We allow heteroatoms in the polymer but consider only cases where a heteroatom is bonded to a carbon atom and not to another heteroatom. Thus, we can tabulate the parameters for each kind of atoms. The relevant parameters are collected in table 1. They could be further optimized for the individual cases.

Table 1

Parameters used in the LHS calculations. N_π is the number of π-electrons per atom. β_0 is the resonance integral for the bond in benzene (r = 1.4 Å).

X	N_π	α/β_0	A (eV)	B (Å)	R_1 (Å)	R_2 (Å)	β_1 (eV)	β_2 (eV)
C	1	0.0	243.5	0.3075	1.54	1.33	−1.626	−3.220
–S–	2	1.5	1938.1	0.2580	1.82	1.71	−1.674	−2.564

However, for comparison of systems within a given family the parameters can be kept fixed, while the accurate values of the parameters are not very critical. The parameters in table 1 have already been tested for many polymers, obtaining good agreement with the results of more sophisticated methods, and experimental results as well, see refs. [20,28,29].

3. Quinoid–aromatic transition in poly-isothianaphthene

Poly-isothianaphthene (PITN) is an interesting polymer because it has the smallest bandgap of about 1 eV in the family of conjugated polymers known so far [14]. Theoretical band calculations using periodic boundary conditions on PITN at the MNDO level showed that this polymer has a quinoidal geometry [30]. MNDO calculations on ITN monomer predicted an aromatic geometry [31]. In a recent comment, we showed that one has to be careful with simply replacing the geometry of a polymer by the geometry of its short oligomer [28].

Our findings can be summarized as follows. The optimum geometry for short chains ($n < 8$, n is the number of unit cells) is aromatic. For long oligomers ($n > 9$), the aromatic character localizes to the chain ends, whereas in the middle one has a quinoidal geometry. These results are collected in fig. 3.

One can see that PITN is an example where small cluster calculations are unacceptable for constructing bulk models of the polymer. Furthermore, our results show an interesting aromatic to quinoidal transition within one ITN oligomer if the chain is longer than 9 monomers.

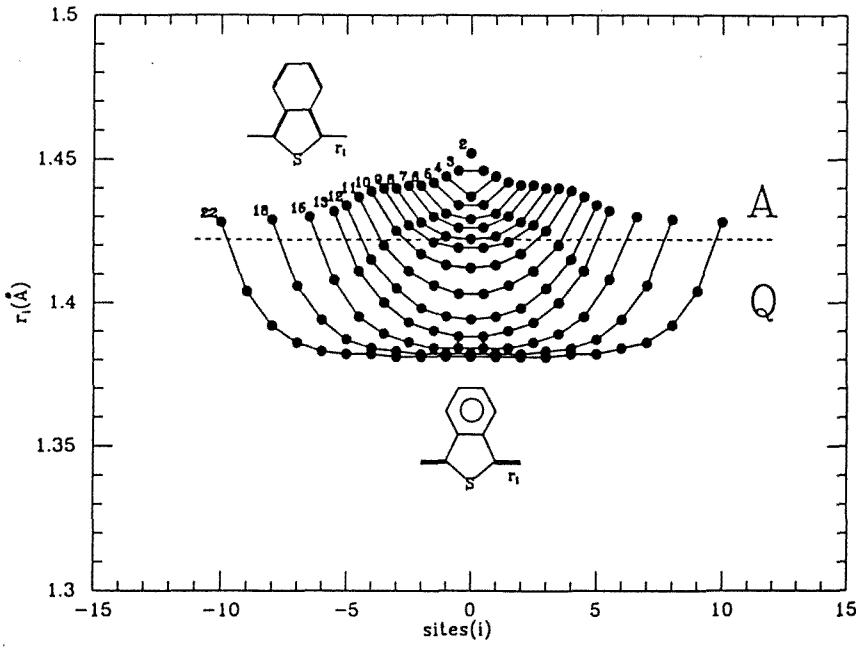

Fig. 3. Variation of optimum bond lengths (r_i) along ITN oligomers with different number of monomers (n). The value of n is indicated by boldface figures. Solid lines are used to connect dots representing bond lengths of a given oligomer. The dashed line separates the aromatic (A) and quinoidal (Q) phases.

These results show an interesting case of embedding. We can focus on the ITN monomer sitting in the middle of the oligomer. For short chains, it has an aromatic geometry which is slowly distorted towards the quinoidal bulk state as the length of the chain increases. The transition takes place at $n = 8$ unit cells. The geometry is then stabilized after $n \approx 20$.

4. Thiophene embedded in polyacetylene

Another interesting example for the embedding problem is provided by the structural changes of a single thiopehene ring connected to two finite or semi-infinite polyene chains.

A related problem, the embedding of phenylene into polyacetylene, was studied by Sautet and Joachim [32] for ortho, meta and para connections. We shall return to this problem in section 6.

The possible connection schemes for thiophene and the two $(CH)_x$ chains are shown in fig. 4. The number of possible cases is larger as compared to phenylene since, in addition to distinguishing between ortho-, meta- and para-type situations, one should specify the positions of the two substitutions relative to the heteroatomic site. Moreover, since the thiophene ring may be in the aromatic or in the quinoidal state, the number of cases is doubled.

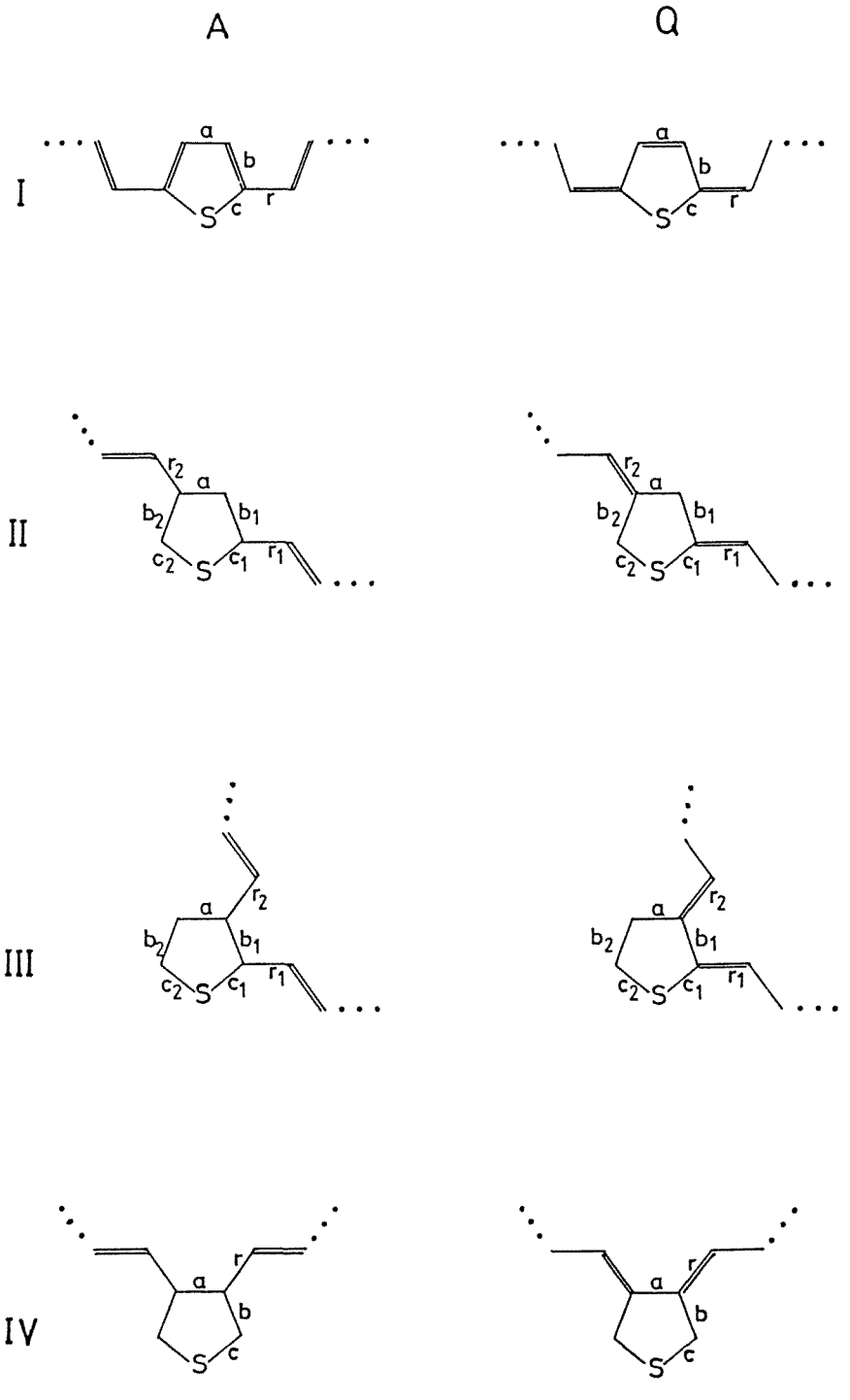

Fig. 4. Possible connection schemes for embedding thiophene into polyacetylene. Column A: aromatic connection; column Q: quinoidal connection.

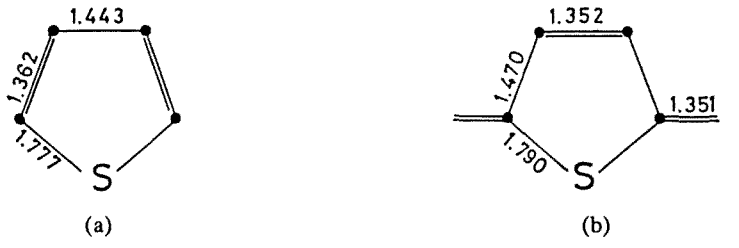

Fig. 5. Optimized bond lengths of thiophene.
(a) Aromatic structure (isolated ring); (b) quinoidal structure.

The optimized structure of an isolated thiophene ring is given in fig. 5(a). This corresponds to the aromatic structure. Forcing the ring to be quinoidal is possible by adding two extra C=C bonds at the two neighbors of the sulfur atom (fig. 5(b)), which corresponds to the case IQ in fig. 4. This form, however, is of significantly higher energy, as is shown by the following consideration. The total energy of the aromatic ring is −48.89 eV. In order to obtain an estimate for the total energy of thiophene in Q form, one may evaluate the π and σ fragment energies by partitioning eq. (3) and eq. (9) in a straightforward manner. In this way, we obtained $E(Q) = -45.54$ eV for thiophene . The thiophene ring thus strongly prefers the aromatic configuration: the stabilization energy is −3.35 eV for the five-bond ring.

The strong preference of the aromatic structure persists even after embedding the thiophene into polyacetylene. Connecting the ring to a pair of chains containing an *even* number of atoms, this will resonate with the tendency of the chains where the alternation is always such that a double bond is formed at the chain ends. For long chains containing 50 atoms, the geometrical characteristics of this situation are shown in table 2. The aromatic character is clearly indicated by r_1 and r_2 being

Table 2

Bond lengths of thiophene embedded into the middle of a chain of 100 atoms. The roman numbers refer to the bonding situations in fig. 4, where the bond identifications a, b_1, b_2, c_1, c_2, r_1 and r_2 are also shown.

	a	b_1	b_2	c_1	c_2	r_1	r_2
I	1.426	1.383	1.778		1.459		
II	1.442	1.375	1.377	1.779	1.774	1.464	1.469
III	1.444	1.391	1.363	1.778	1.777	1.456	1.461
IV	1.454	1.377	1.775		1.468		

always single bonds. They are larger than 1.45 Å in each case. The geometry of the polyene chain becomes more interesting if it consists of an *odd* number of atoms on both sides. Then, as a double bond is always formed at the chain end, there will

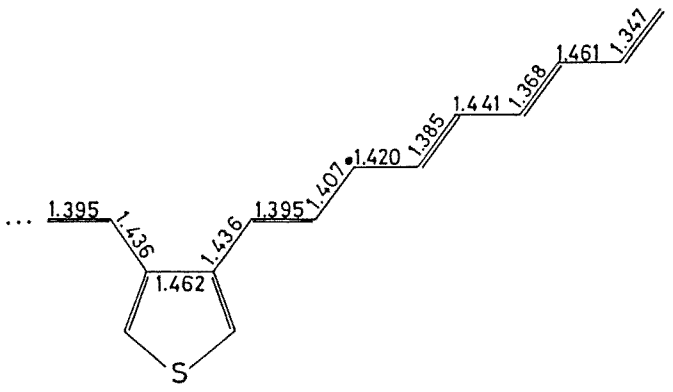

Fig. 6. Thiophene in the middle of a $(CH)_{18}$ chain.

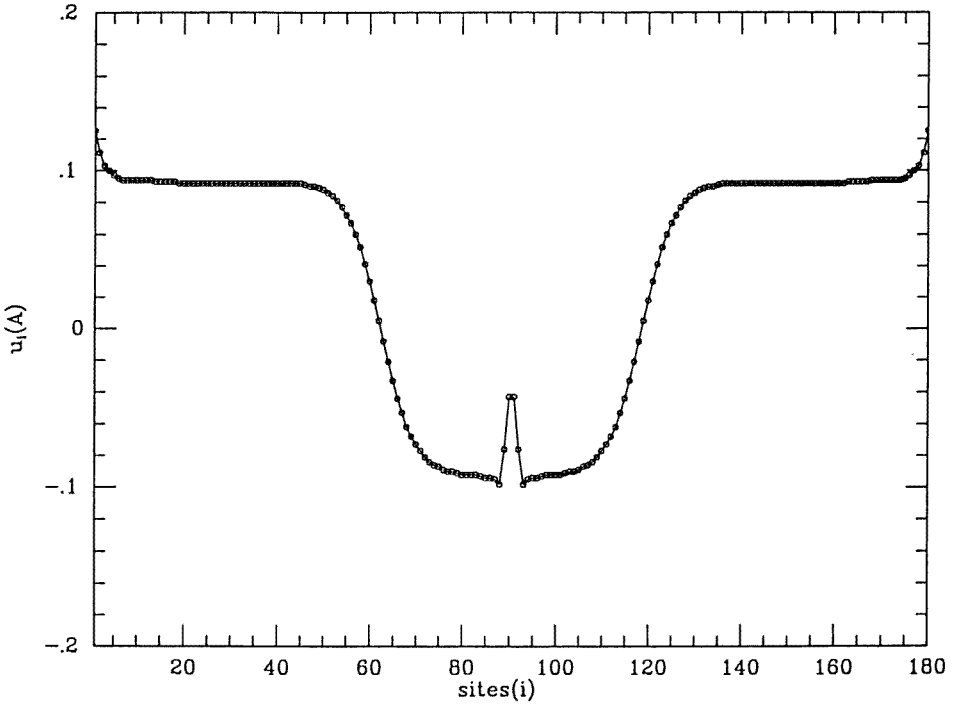

Fig. 7. The alternation pattern of a system composed of a thiophene ring and two C_{89} chains according to bonding scheme I in fig. 4. The alternation is defined by $u_i \equiv (-1)^{i+1}(r_{i+1} - r_i)$.

be a competition between this tendency and the aromatic preference of the ring. For very short side segments, e.g., containing one to three atoms, the odd chain will force the ring to take a quinoidal structure. Such an example was shown in fig. 5(b).

The situation is similar for other bonding situations, too. For side chains having a medium (odd) number of atoms, e.g., 9 on both sides, the A or Q nature of the ring depends on the specific bonding situation. In cases I and III, the ring is in Q form, while in cases II and IV the A form is stabilized. Case IV is shown in fig. 6. This feature still persists even for 51 carbon atoms in the side chains. The A-type rings with odd side chains necessarily generate a phase kink ("soliton") in the polyene chain. However, for long enough side chains the thiophene ring always appears in the A form and solitons are generated on the chain independently of the bonding situation. Figure 7 shows the alternation pattern of a $(CH)_{178}$ chain with a thiophene sitting in the middle.

We see that independently of the parity of the side chains, an embedded thiophene in polyacetylene always appears in the A form. Thus, the ring acts as a boundary condition for the two sides of the polymer. If there is a mismatch between the alternation patterns required by the A ring and the chain ends, a pair of solitons is generated along the chain whose creation energy is thus smaller than the A–Q stabilization energy, 3.35 eV, as calculated above.

5. Thianaphthene embedded in polyacetylene

We have seen in the previous section that the aromatic preference of thiophene in polyacetylene was strong enough to modify the geometry of the embedding chains rather than to change its own state. In this section, we shall consider a different situation: the embedding of thianaphthene. This molecule can also be in an aromatic or quinoidal state (fig. 8), but the energy separation between these two

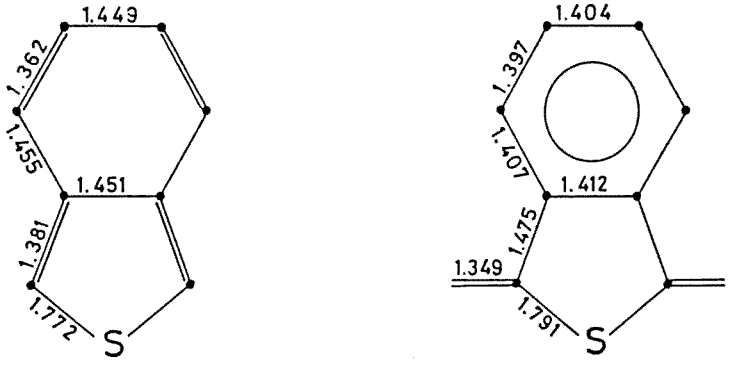

Fig. 8. The aromatic (a) and quinoidal (b) form of thianaphthene.

states, as evaluated in our model, is only 2.81 eV. Comparing this energy to the A–Q stabilization energy of thiophene, 3.35 eV, we see that the A form for thianaphthene is stabilized to a much lesser extent. This will have remarkable consequences: an embedded thianaphthene will not serve as a boundary condition

in the $(CH)_x$ chain, but it will adapt to the bond length alternation pattern forced by the chain by being excited to Q or relaxing to the A state, depending on the parity of the number of C atoms in the side chains.

These considerations are fully supported by the numerical calculations on the geometrical parameters of embedded thianaphthene presented in fig. 9.

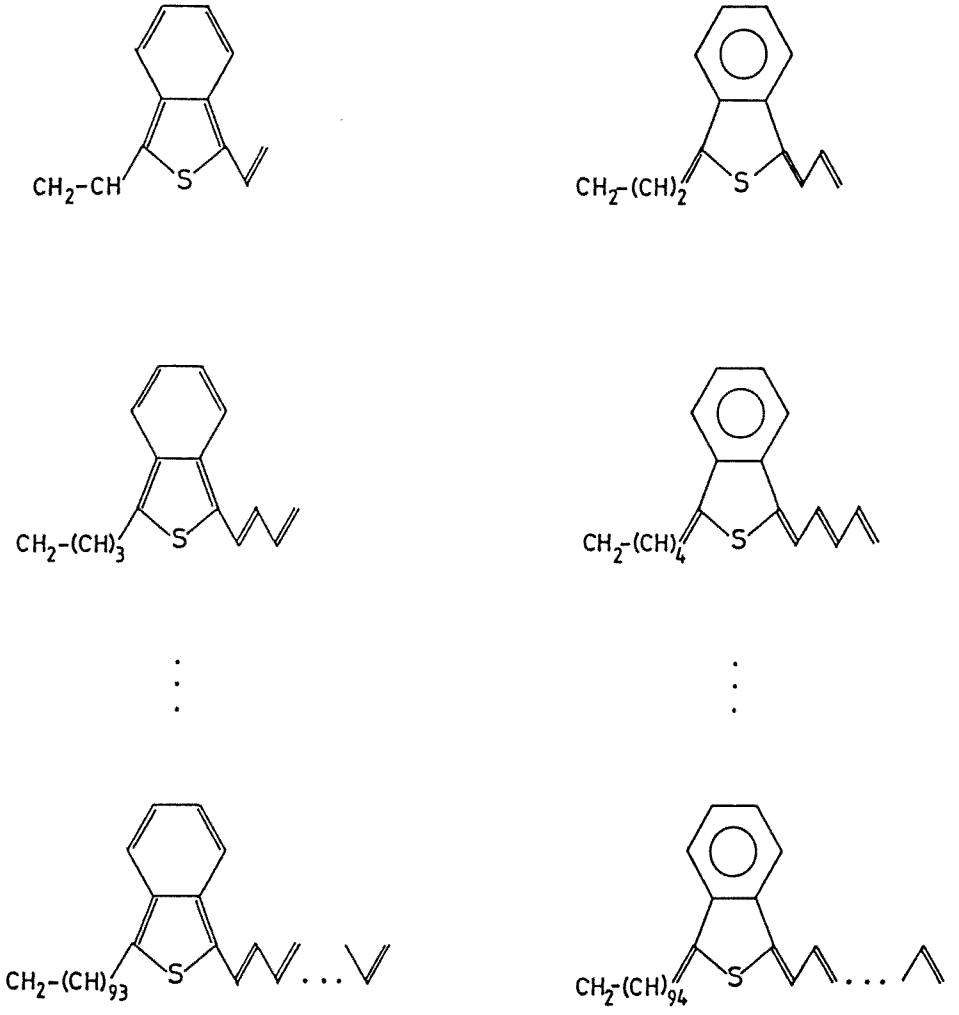

Fig. 9. Schematic structure of thianaphthene embedded in polyenes; only case I of fig. 4 is considered. The structure is aromatic (A) or quinoidal (Q) for chains with even or odd numbers of C atoms, respectively.

The previous examples provided illustrations to short- and long-range effects for the embedding problem. In section 4, we found that a Q → A transition of the structure of the embedded unit may take place either for relatively short side chains

(short-range interaction), or only for long chains, depending on the specific bonding situation. For example, in case I of fig. 4, transition occurs between $n = 51$ and $n = 89$, n being the number of atoms in the side chain. This represents a typical long-range interaction.

In the present section, we can see other examples for long-range interactions. Owing to the relatively small energy separation between the A and Q forms, any additional atom changes the structure of the embedded unit, even for very long chains. In other words, the structure of the embedded thianaphthene is sensitive to the chain length: it takes the Q form for odd n and the A form for even n.

It has to be emphasized that some conclusions drawn above may be valid only within the present model of calculation. This is expected to be the case when degeneracy occurs at the Fermi level.

6. Embedded defects: conjugation interruption

The basic question we have investigated so far was the effect of the environment on the structure of an embedded unit. However, the problem can be considered from a reverse point of view: one can study the changes in the structure of the host medium due to an embedded "defect".

Several types of defects in polyacetylene can be considered. Here, we shall consider them from a specific point of view: we shall investigate to what extent these defects interrupt the conjugation in the $(CH)_x$ chain.

As mentioned already, the case of embedded phenylene was studied recently by Sautet and Joachim [32]. They also investigated the dynamics of the problem and defined a transmission coefficient characterizing the interruption of conjugation. They found that the meta connection destroys the conjugation to a large degree, while the electron transmission in the ortho and para case is much better. The smallest conjugation interruption was shown in the para situation.

To investigate this problem, we have used an η conjugation interruption parameter defined previously [18,19]:

$$\eta = \frac{\Delta E_{\mathrm{def}}}{\Delta E_{\mathrm{cut}}}. \tag{14}$$

Here, ΔE_{def} and ΔE_{cut} describe the increase of the first excitation energy of a chain due to a given defect or due to a cut of the chain at the same site, respectively. Calculating the conjugation interruption parameter, we obtained $\eta = 89\%$, 73% and 62% for the meta, ortho and para case, respectively. This is in full agreement with the results of Sautet and Joachim. We have also evaluated the geometry of an embedded phenylene ring in ortho, meta and para forms. The results are shown in fig. 10.

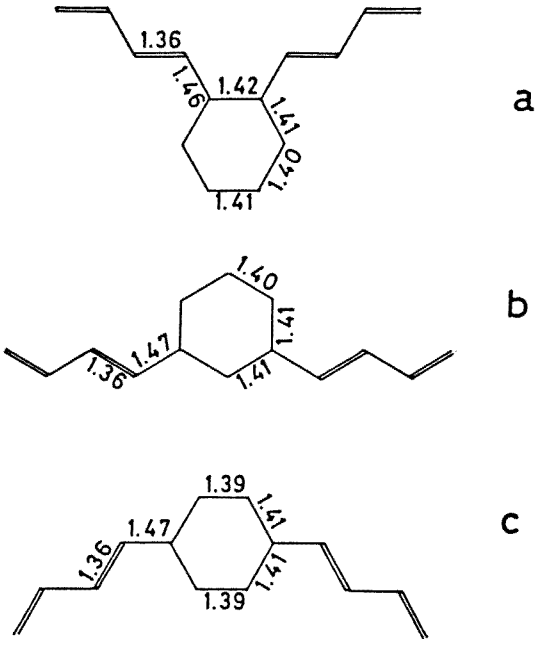

Fig. 10. The geometry of a phenylene ring embedded in polyacetylene in ortho (a), meta (b), and para (c) forms.

Acknowledgements

Discussions with Professor M. Kertész are gratefully acknowledged. This research was supported in part by Grant No. OTKA 64/1987 and in part by Grant No. OTKA 517/1990.

References

[1] *Proc. Int. Conf. on Science and Technology on Synthetic Metals*, Tübingen, Germany (1990), Synth. Metals 41–43.
[2] H. Kuzmany, M. Mehring and S. Roth (eds.), *Electronic Properties of Conjugated Polymers I–III*, Springer Series in Solid-State Sciences, Vols. 66, 76, 91 (1985–87–89).
[3] T.A. Skotheim (ed.), *Handbook of Conducting Polymers* (Marcel Dekker, New York, 1986).
[4] J. Simon and J.J. André, *Molecular Semiconductors* (Springer, Berlin, 1985).
[5] M. Kertész, Adv. Quant. Chem. 15(1982)161.
[6] C.K. Chiang, C.R. Fincher, Y.W. Park, A.J. Heeger, H. Shirakawa, E.J. Louis, S.C. Gau and A.G. MacDiarmid, Phys. Rev. Lett. 39(1977)1089.
[7] J.C.W. Chien, *Polyacetylene, Chemistry, Physics and Material Science* (Academic Press, Orlando, 1984).
[8] H. Naarmann and N. Theophilu, Metals 22(1987)1.
[9] J. Tsukamoto and A. Takahashi, Metals 41(1991)7.
[10] R.E. Peierls, *Quantum Theory of Solids* (Clarendon, Oxford, 1955).

[11] W.P. Su, J.R. Schriffer and A.J. Heeger, Phys. Rev. B22(1980)2099.
[12] C.R. Fincher, C.E. Chen, A.J. Heeger, A.G. MacDiarmid and J.B. Hastings, Phys. Rev. Lett. 48(1982)100.
[13] T.C. Clarke, R.D. Kendrick and C.S. Yannoni, J. de Phys. 44, C3(1983)369.
[14] F. Wudl, M. Kobayashi, N. Colaneri, M. Boysel and A.J. Heeger, Mol. Cryst. Liq. Cryst. 118(1985)199; M. Kobayashi, N. Colaneri, M. Boysel and A.J. Heeger, J. Chem. Phys. 82(1985)5717.
[15] M. Kertész and P.R. Surján, Sol. Stat. Commun. 39(1981)611.
[16] P.R. Surján, H. Kuzmany and K. Iwahana, in: *Phonon Physics*, ed. J. Kollár, N. Kroó, N. Menyhárd and T. Siklós (World Scientific, Singapore, 1985).
[17] P.R. Surján, A. Vibók, H. Kuzmany and K. Iwahana, Springer Series in Solid State Science, Vol. 63 (1985), p. 133.
[18] P. Surján and H. Kuzmany, Phys. Rev. B33(1986)2615.
[19] J. Kürti and H. Kuzmany, Springer Series in Solid State Sciences, Vol. 76 (1987), p. 43; Phys. Rev. B38(1988)5634.
[20] J. Kürti and P.R. Surján, Springer Series in Solid State Sciences, Vol. 91 (1989), p. 69.
[21] J. Kürti and H. Kuzmany, Phys. Rev. B44(1991)597.
[22] H.C. Longuet-Higgins and L. Salem, Proc. Roy. Soc. A251(1959)172.
[23] R. Pariser and R.G. Parr, J. Chem. Phys. 21(1953)767.
[24] C.A. Coulson, Proc. Roy. Soc. London A207(1951)91.
[25] A. Julg, G. Del Re and V. Barone, Phil. Mag. 35(1977)517; A. Julg, Lecture Notes in Chemistry, Vol. 9 (Springer, Berlin, 1978).
[26] I. László and A. Julg, Acta Phys. Hung. 58(1985)199.
[27] G. Biczó, L. Polgár and M. Tomasek, Phil. Mag. A56(1987)285.
[28] J. Kürti and P.R. Surján, J. Chem. Phys. 92(1990)3247.
[29] J. Kürti, P.R. Surján and M. Kertész, J. Amer. Chem. Soc. 113(1992)9865.
[30] Y.S. Lee and M. Kertész, J. Chem. Phys. 88(1988)2609.
[31] J.L. Br´das, A.J. Heeger and F. Wudl, J. Chem. Phys. 85(1986)4673.
[32] P. Sautet and C. Joachim, Chem. Phys. Lett. 153(1988)511.